Iridescent structural colour production in male blue-black grassquit feather barbules: the role of keratin and melanin

Rafael Maia[1,2,*], João Victor O. Caetano[3], Sônia N. Báo[3] and Regina H. Macedo[1]

[1]*Laboratório de Comportamento Animal, Departamento de Zoologia, and* [2]*Programa de Pós-Graduação em Ecologia, Universidade de Brasília, Brasília 70910-900, Brazil*
[3]*Laboratório de Microscopia Eletrônica, Departamento de Biologia Celular, Universidade de Brasília, Brasília 70919-970, Brazil*

Iridescent coloration plays an important role in the visual communication system of many animal taxa. It is known that iridescent structural colours result from layers of materials with different refractive indexes, which in feathers usually are keratin, melanin and air. However, the role of these materials in the production of structural iridescent coloration is still poorly documented. Despite the great interspecific variation in the organization of such structures in bird plumage, melanin layers are usually considered too opaque, suggesting its main role is to delineate the outermost keratin layer and absorb incoherently scattered stray light. We combined spectrometry, electron microscopy and thin-film optical modelling to describe the UV-reflecting iridescent colour of feather barbules of male blue-black grassquits (*Volatinia jacarina*), characterized by a keratin layer overlying a single melanin layer. Our models indicate that both the keratin and the melanin layers are essential for production of the observed colour, influencing the coherent scattering of light. The melanin layer in some barbules may be thin enough to allow interaction with the underlying keratin; however, individuals usually have, on an average, the minimum number of granules that optimizes absorbance by this layer. Also, we show that altering optical properties of the materials resulted in better-fitting models relative to the empirically measured spectra. These results add to previous findings concerning the influence of melanin in single-layer iridescence, and stress the importance of considering natural variation when characterizing such photonic structures.

Keywords: barbule; feather; sexual selection; photonic crystal; thin film; visual communication

1. INTRODUCTION

Visual signals play a major role in avian communication, inferred from the keen colour discrimination (Cuthill 2006; Håstad & Ödeen 2008) and the diversity and ubiquity of ornaments and colorations found in this taxon (Andersson 1994). Coloration properties of secondary sexual traits may provide reliable information about an individual's genetic quality (Figuerola *et al.* 1999), aggressiveness (Alonzo-Alvarez *et al.* 2004) or reproductive strategy (Badyaev & Hill 2002), which may be used by individuals during agonistic or mate choice interactions (Searcy & Nowiki 2005).

Traditionally, mechanisms for production of feather coloration have been subdivided into two categories. Pigmentary colours result from the chemical properties of pigments and their concentration in feathers, which allow the differential absorption and reflectance of light of different wavelengths. The chief pigments in this category are carotenoids, which produce red, orange and yellow coloration, and melanins, responsible for black, brown and rufous colours (McGraw 2006*a,b*). Although these pigments may combine to produce several other hues, they are not responsible for all known avian colorations—for example, no known pigments produce blue coloration (Bagnara *et al.* 2007), and only rarely do they produce green coloration (McGraw 2006*c*).

Structural colours are an alternative path to colour production and rely on the organization and differential refraction properties of the nanostructures that compose feathers, producing an astonishing array of green, blue, violet and ultraviolet tones (Kinoshita *et al.* 2008).

The most common materials in these structures are keratin, melanin (in the form of granules, called melanosomes) and air (Prum 2006).

The ultraviolet component of the spectrum is invisible to the human eye. However, several studies, ranging from behavioural and electrophysiological data to opsin coding of UV-absorbing cone genes, have indicated that most birds have tetrachromatic vision and can see light in the ultraviolet spectrum (Cuthill *et al.* 2000; Cuthill 2006). It remains controversial whether light in this spectrum represents a special communication channel for birds or whether it is just another chromatic channel (Banks 2001; Haussmann *et al.* 2003). In either case, the universality of colour production in this range (Eaton & Lanyon 2003), and therefore the role of feather nanostructures in the production of this colour component, should not be underestimated.

Structural coloration is usually produced by coherent scattering of light, in which refractive particles are organized in size, shape and distribution in a manner that promotes a non-random interaction of different refracting wavelengths. Certain wavelengths may be in phase after interacting with the structure (interfering constructively and being reinforced), while others will be out of phase (and will thus interact destructively), resulting in the observed colour (Kinoshita & Yoshioka 2005*a*). These structures may be organized in one, two or even three dimensions (Prum & Torres 2003).

In feather barbules, unidimensional (i.e. thin film) and bidimensional structures have been described (e.g. Greenwalt *et al.* 1960; Prum *et al.* 1998; Andersson 1999; Zi *et al.* 2003), and recent techniques have provided new insights indicating that three-dimensional photonic structures may also be found in the medullar cortex of feather barbs (Shawkey *et al.* in press). Structures organized in one and two dimensions have the additional feature of being iridescent, i.e. changing colour properties (especially hue) as a function of the angle of light incidence (Osorio & Ham 2002). This characteristic derives from the coherent refraction of light through laminar structures, in which angle affects the optical distance (a function of linear distance and refractive index) that light will encounter, therefore altering the phase relations in each refracted wavelength (Kinoshita & Yoshioka 2005*b*).

Barbule nanostructures may be found in various unidimensional organizations to produce iridescence, resulting in great interspecific variability of structures and colours. For example, a thick, absorbing melanin layer underlying a keratin cortex results in violet-blue coloration, as found in the velvet satin bowerbird (*Ptilonorhynchus violaceus minor*; Doucet *et al.* 2006) and some blackbirds and grackles (Shawkey *et al.* 2006). However, iridescent structural colours can be obtained without the influence of a melanin layer in coherent scattering, as appears to be the case of the rock dove (*Columba livia*), where melanin granules are considerably larger and randomly dispersed (Yoshioka *et al.* 2007). In this species, the green-violet iridescence can be modelled as the product of a thin layer of keratin in an air substrate (Yin *et al.* 2006; Yoshioka *et al.* 2007). However, even in such cases, melanin can play an important role by acting as a poor mirror, resulting in higher peak reflectance and overall brightness

(Yin *et al.* 2006), by absorbing incoherently scattered light, and by structurally defining the width of the keratin layer during the developmental process (as suggested by Doucet *et al.* 2006). Nonetheless, both air and melanin may interact with keratin in multilayer stacks to produce very bright iridescent coloration of multiple hues, typically observed in hummingbirds (Greenwalt *et al.* 1960).

Thin-film optical modelling is a very useful tool to study animal iridescent coloration, allowing predictions concerning the behaviour of light when interacting with colour-producing structures, based on nanomorphological and optical properties; such predictions may then be compared with the spectra obtained from the biological structures (Shawkey *et al.* 2006; Yoshioka *et al.* 2007). Furthermore, thin-film optical modelling allows the manipulation of optical properties to test for their adequacy in characterizing these structures (Brink & van der Berg 2004; Doucet *et al.* 2006). Despite these advantages, two major methodological obstacles have hindered biologists pursuing an integrative approach: the lack of a simple operational tool to apply the necessary calculations for the models; and an objective way of comparing the predicted and obtained spectra, which is usually done visually and does not allow a fine-scale fit to the model.

The blue-black grassquit (*Volatinia jacarina*) is a small neotropical emberizid in which morphological and behavioural characteristics are interrelated in a complex communication process during social interactions. During the breeding season, males moult to a blue-black iridescent structural coloration, while females maintain a cryptic plumage. Males defend small, clustered territories by repeatedly performing vertical leaping displays, during which their conspicuous plumage is exhibited to conspecifics in a variety of angles of incident light (Webber 1985). Though the role of plumage coloration in social interactions remains unexplored, coloration characteristics of this species have been shown to be condition dependent (Doucet 2002), and both the amount of nuptial plumage and display characteristics are related to parasite load (Costa & Macedo 2005; Aguilar *et al.* 2008).

It is very likely that visual communication in this species, especially relative to plumage, is important in social interactions, and may play a role in the high rate of extra-pair copulation that has been documented (Carvalho *et al.* 2006). Hence, the blue-black grassquit provides a potentially excellent model system to study both proximate and evolutionary mechanisms that promote the production and maintenance of iridescent coloration. In this study, we identify the mechanisms of structural colour production of male blue-black grassquits. To accomplish our objective, we combined spectrometric measurements, transmission electron microscopy (TEM) to characterize the nanostructures of feather barbules and thin-film modelling. We further investigate the role of optical properties of these structures, identifying the effects of altering these parameters upon coloration. For this purpose, we developed a routine based on open access software, a tool that can be widely applied to studies of the mechanisms of iridescent structural colour production.

2. MATERIAL AND METHODS

2.1. Sampling

We captured and banded birds in the Fazenda Água Limpa (property of Universidade de Brasília), Brazil (15°56′ S, 47°56′ W) during the breeding seasons of November–January 2005–2006 and 2006–2007. We plucked three feathers from various body parts of males, but for the present analyses we used only dorsal feathers. If individuals were moulting, we only collected feathers clearly identifiable as nuptial plumage. All feathers were taped to a black card and individually identified, wrapped in foil paper and kept in the laboratory under dry and stable temperature conditions.

2.2. Colour measurement

For colour measurements, feathers were taped in an overlaid manner to a black velvet substrate to simulate their arrangement on the bird's body. Feather reflectance was measured with an Ocean Optics USB4000 spectrometer attached to a PX-2 pulsed xenon light source (range 250–750 nm, Ocean Optics, Dunedin, FL). All measurements were taken with R400-7 UV-VIS optic fibre reflection probes (400 μm diameter), using unpolarized light and relative to a WS-1-SS white standard (Ocean Optics).

To characterize iridescence, reflectance measurements were taken from two measurement geometries: using a bifurcated optic probe held perpendicular to the feather surface (hereafter 'normal geometry', since both light source and observer are parallel to the feather surface normal), and with probe ends at separate angles of illumination and measurement, specularly positioned at 45° from the normal (hereafter, '45°'). These measurement geometries were selected because a pilot study indicated that they provide reliable information on overall iridescent behaviour of the coloration, offering the most saturated and repeatable measurements. Optic fibres were held using a block sheath to exclude ambient light and to maintain the optic probes 6 mm from the feather surface. We used SPECTRASUITE software (Ocean Optics) to record and measure 50 sequential spectra from the feathers with an integration time of 20 ms, and this procedure was repeated five times for each sample. Between repetitions, to guarantee that different parts of the feather surface were sampled, we lifted the sheath from the feather surface before positioning it for the new measurement. All measurements were interpolated to a step width of 1 nm, and calculations were performed based on the average spectra of these five repetitions, from 320 to 700 nm.

2.3. Transmission electron microscopy

We prepared three whole barbs from dorsal feathers of each male for TEM (protocol modified from Andersson 1999). Barbs were immersed for 30 min in a 0.25 M NaOH solution and for 2 hours in formic acid : ethanol (2 : 3 v/v). After bathing in distilled water, they were dehydrated in acetone in increasing concentrations (15 min in 30, 50, 70 and 90 per cent, and three 10-min immersions in pure acetone). Inclusion was carried out
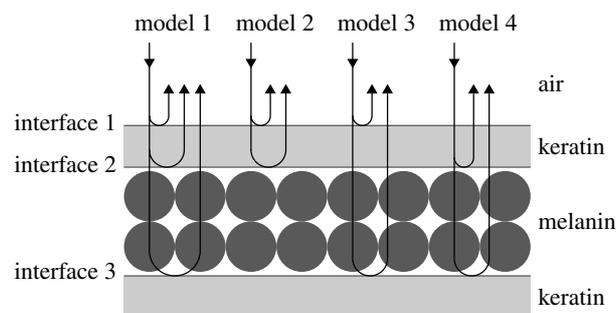

Figure 1. Schematic of all thin-film optical models considered in this study. Arrows represent incident and reflected beams of light.

in increasing solutions of Spurr resin and acetone (3 : 1, 2 : 1, 1 : 1, 1 : 2 and 1 : 3, overnight in odd steps and for 6 hours in even steps, finalizing in pure Spurr for 6 hours). Barbules were then placed in Spurr blocks and allowed to polymerize at 60°C. Preliminary analyses revealed that the keratin matrix and the melanosomes were sufficiently electron dense, and thus no contrasting was conducted to avoid depositing residues in the material.

Polymerized blocks including barbules were cut using a diamond knife on a Leica Reichert Supernova ultramicrotome (Leica Microsystems, Austria). Sections were placed in 150 mesh grids and observed in a JEOL JEM-1011 TEM (80 kV; JEOL, Japan). We obtained micrographs at 10 000× magnification from three barbules from the distal portion of different barbs for each individual. Images were obtained with a digital camera and digitally magnified for a final 25 000× magnification. From these images, we obtained three nanostructural measurements at six equidistant points for each barbule: keratin cortex thickness; outer melanin layer thickness; and number of granules in the outer melanin layer. Melanin granule diameter was estimated by dividing melanin layer thickness by the number of granules in the section measured. We used the mean of the six measurements of the three barbules to characterize each individual. All measurements were taken using IMAGEJ v. 1.38x (Rasband 1997–2007, available at http://rsb.info.nih.gov/ij/index.html).

2.4. Models of colour production

We used thin-film optical modelling to characterize and identify the influence of structures in colour production. Our main objective was to identify the best-fitting model to the observed spectra, considering the importance of keratin and melanin layer properties obtained from TEM. We used the transfer matrix method (see Jellison 1993) to create four models, as described below. Since we used unpolarized light in all measurements, the s and p components of polarization were averaged (Srinivasarao 1999).

To identify the influence of each component structure in the production of blue-black grassquit iridescent coloration, we considered four models that define all possible two- and three-beam combinations of interfaces produced by a set of two overlapping layers (figure 1; for more details, see Doucet *et al.* 2006;

Shawkey *et al.* 2006). Model 1 takes into account all three interfaces and the thickness of both layers. Model 2 takes into account the two outermost interfaces and the keratin cortex thickness. Model 3 takes into account the two outermost interfaces and the thickness of the melanin layer, thus considering that keratin thickness does not influence the optical distance of the layer (i.e. considered transparent). Finally, model 4 takes into account only the two innermost interfaces and the thickness of the second layer, once again considering the keratin layer transparent. Although model 1 is the only model that does not exclude any structures deemed relevant, combining these models allows conjectures about the relative importance of each layer to colour production, since we can assess the effects of removing individual components on the produced spectra.

In all the models, the melanin layer was considered to be immediately below and parallel to the keratin layer, ultimately defining its width. For simplicity, all models were generated considering smooth layers. We initially considered published estimates of real refractive indexes (n) and extinction coefficients (k) of air ($n=1.00$, $k=0.00$), keratin ($n=1.56$, $k=0.03$) and eumelanin ($n=2.00$, $k=0.6$) in all calculations (Land 1972; Brink & van der Berg 2004). Since spectra obtained from these models are very disparate, we visually compared model fit to the observed data (Brink & van der Berg 2004; Doucet *et al.* 2006; Shawkey *et al.* 2006).

All models were calculated using a script developed for R software (R Development Core Team 2007; available at http://cran.r-project.org). This user-friendly script is a valuable tool for the integrative study of animal structural coloration, as it allows the calculation of any combination of layers and refractive indexes, as well as the four predefined models considered in this study. The programming code is available in the electronic supplementary material or upon author request.

We considered the observed spectrum as the average of the measured spectra of all individuals, and all models used the average measurements from nanostructures of these individuals. Since barbule tilting relative to the feather axis may produce differences in measured brightness (Osorio & Ham 2002), all comparisons were made with spectra normalized to have integrals of 1. We selected the best general model through visual inspection. However, since we had a considerably larger sample size compared to similar studies, we calculated the 95% confidence intervals (CIs) for the estimates of hue mean, for both normal and 45° geometries, and also for the estimate of hue shift with geometry owing to iridescence ($\Delta\mathrm{Hue}=\mathrm{Hue}_{90}-\mathrm{Hue}_{45}$). We used the obtained intervals to estimate goodness of fit from models with subtle differences owing to changes in optical properties of the component structures. Although a similar approach has been used to assess the model fit to observed reflection in the Madagascan sunset moth (Yoshioka *et al.* 2008), the use of CIs allows for some uncertainty of the calculated values owing to both natural variation and measurement accuracy, therefore providing a more conservative and biologically relevant estimate of model adherence.
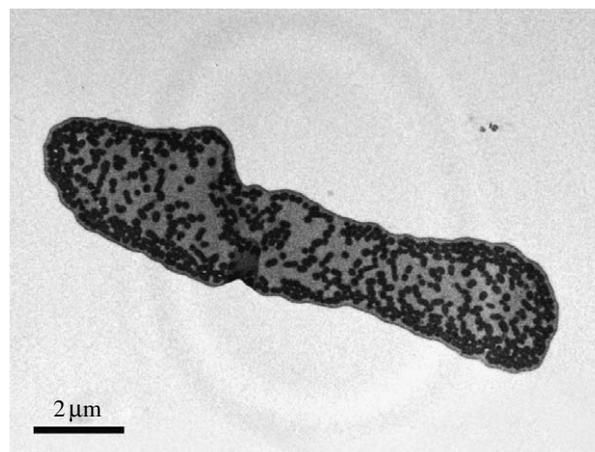

Figure 2. Transmission electron micrograph of a representative barbule from a dorsal feather of the nuptial plumage of male blue-black grassquits (magnification 10 000×). Black ovals are melanin granules and dark grey areas are keratin.

Table 1. Nanostructural measurements of male blue-black grassquit feather barbules, obtained from TEM. (Each sample corresponds to the average of six measurements from three barbule micrographs of different feathers of the same individual.)

variable	mean ± s.e.m. ($n=25$)
keratin cortex thickness (nm)	126.57 ± 2.08
melanin layer thickness (nm)	421.76 ± 12.29
melanin granules in layer	2.45 ± 0.06
melanin granule diameter (nm)	177.69 ± 5.17

3. RESULTS

3.1. Barbule microstructure

We obtained and measured 75 micrographs from barbules of 25 adult male blue-black grassquits. Although melanin granules were also found scattered within the matrix, several were distributed and organized in a seemingly discrete layer, beneath a thin and uniform keratin layer (figure 2).

Our measurements revealed that the keratin cortex is thinner than the outer melanin layer, with the latter comprising one to five melanin granules in thickness (table 1). Although this melanin layer was usually thicker than one granule, we never observed keratin–melanin layer stacks (i.e. sequences of discrete keratin and melanin layers). Furthermore, the distance between the melanin granules in this outer layer was consistently lower than 300 nm, therefore not allowing individual interaction with light in all avian visible wavelengths (300–700 nm; Cuthill *et al.* 2000) and conferring an organization typical of single-layer thin-film optical systems.

3.2. Spectrometric measurements

The colour spectra obtained from the measurements of the same 25 feathers that were analysed nanostructurally were characterized by a single peak in the range of avian visible wavelengths (figure 3). Changes in the
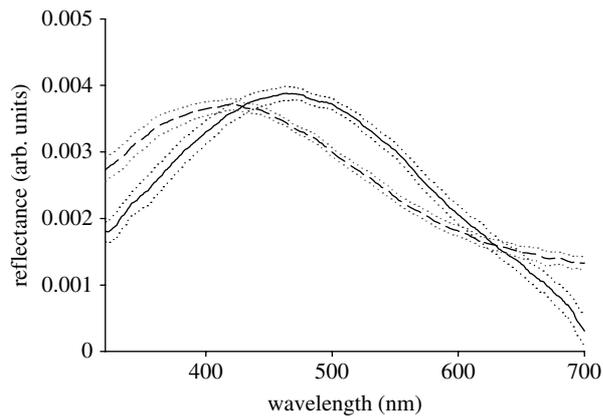
Figure 3. Reflectance spectra of feathers from the nuptial plumage of male blue-black grassquits measured at normal (solid line) and 45° (dashed line) measurement geometries (dotted lines = 95% CI; $n = 25$).

Table 2. Average values and estimated confidence limits for the hue of reflectance spectra obtained from feathers of male blue-black grassquits at two different measurement geometries, and for the difference in hue between those two measurements (ΔHue).

measurement geometry ($n = 25$)	mean (nm)	95% CI	
		lower limit (nm)	upper limit (nm)
normal	464.2	455.8	473.3
45°	413.4	403.4	423.3
ΔHue	51.2	44.2	58.1

measurement geometry shifted the wavelength of peak reflectance, such that an increase in the angle of incidence produced a decrease in hue. There was no overlap in the CI estimates of mean hue at both measured geometries (table 2).

3.3. Thin-film optical modelling

Two of the models considering the outer melanin layer (models 1 and 2 in figure 4a,b) resulted in spectra similar to the ones measured empirically. The shape of the curve and the hue of the modelled spectra had a good fit relative to the spectra measured at both measurement geometries, and both modelled and measured curves had similar behaviour with the changing angle of light incidence, with hues shifting to shorter wavelength and more saturated spectra (i.e. greater spectral purity) owing to the increase in the angle of incidence relative to the normal. Therefore, the disposition of melanin granules in an organized fashion seems indispensable for the production of the observed colour by coherently scattering light.

Model 2 does not consider the width of the melanin layer or the fact that light reaches the interface between the melanin layer and the keratin matrix beneath it. Hence, the similar behaviour of models 1 and 2 (resulting in nearly identical curves in figure 4a,b) reveals that the melanin layer has isolating properties. Models 3 and 4, which do not consider the keratin
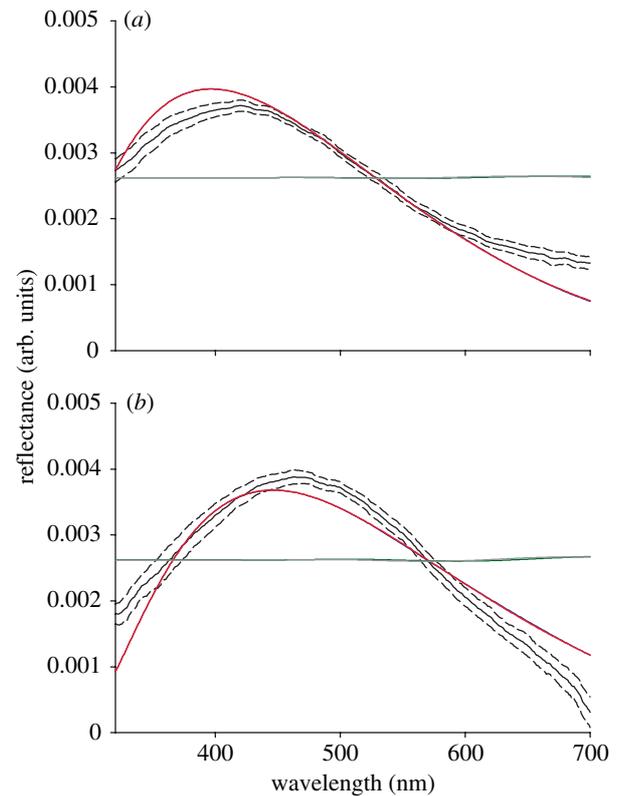

Figure 4. Comparison of the reflectance spectra of feathers from the nuptial plumage of male blue-black grassquits (black solid line, mean; black dashed lines, 95% CI) and the predicted spectra from the four models (blue, model 1; red, model 2; green, model 3; grey, model 4) based on average measurements of barbule nanostructures ($n = 25$) at (a) normal and (b) 45° measurement geometries.

cortex width, resulted in very different spectra from the ones measured from blue-black grassquit feathers, therefore highlighting the importance of the keratin cortex to the production of the observed colour.

Owing to the considerable inter-individual variation in the number of granules composing the melanin layer (figure 5a), which consequently affects the layer width, we ran alternative versions of model 1, with varying widths of the melanin layer based on granule diameter and number of granules, to identify the effect of this variation upon the resulting spectra. We considered that the difference in the number of granules resulted from differences in the deposition of granules from the keratin medulla to the melanin layer, therefore affecting melanin layer width but not keratin layer width. Based on the average granule diameter, only two melanin granules sufficed to isolate the keratin cortex from the core of the barbule, since model 1 converges to model 2 when a two-granule-thick melanin layer is used (figure 5b). However, this also indicates that, considering an average keratin cortex thickness, a one-granule-thick melanin layer can be penetrated by light, which interacts with the second melanin–keratin interface and produces a colour spectrum with hue shifted to longer wavelengths relative to a similar barbule with a two-granule-thick melanin layer.

Despite these procedures, we still found some small-scale differences between the observed and modelled spectra that could not be explained by variation in the
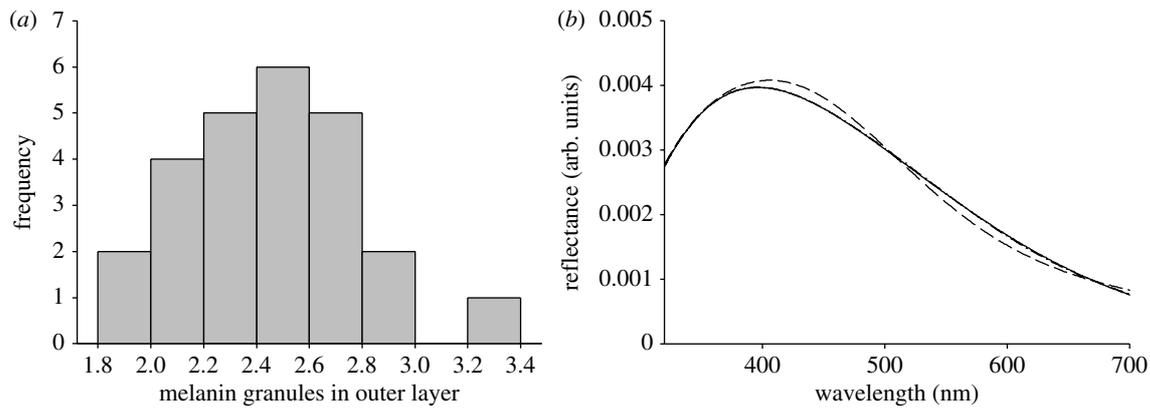
Figure 5. (*a*) Frequency distribution of the average number of melanin granules in each individual's melanin layer and (*b*) predicted spectra for a barbule with an average-width keratin layer measured for male blue-black grassquits, with total isolation by the melanin layer (solid line, model 2) and considering a melanin layer of thickness of one (dashed line) or two (dot-dashed line) average-sized melanin granules.

Table 3. Predicted values of hue and hue shift with measurement geometry (ΔHue) obtained from selected models considering different values of melanin opacity. (Values in italics indicate hues that fall within the 95% CI shown in table 2.)

model optical properties		angle of light incidence		
refractive index (n)	extinction coefficient (k)	normal (nm)	45° (nm)	ΔHue (nm)
2.0	0.6	447	396	*51*
	0.4	437	384	*53*
	0.8	453	402	*51*
1.8	0.6	*466*	*414*	*52*
	0.4	453	*406*	*47*
	0.8	*470*	*417*	*53*
2.2	0.6	432	385	*47*
	0.4	420	377	*43*
	0.8	440	391	*49*

variables considered. A comparison of the initially modelled spectra and the empirically obtained estimates indicates that hue values do not fall within the 95% CI limits (table 3). Therefore, we investigated whether the changes in keratin and melanin opacity would affect the goodness of fit of the modelled spectra relative to the measured one by running the thin-film models with a broad range of refractive index and extinction coefficient values.

Considerable changes to the extinction coefficient of both keratin and melanin did not improve the predictive ability of the thin-film models (figure 6*a*,*b*, dashed lines). However, relatively small changes to the refractive index of both materials resulted in models with a better fit. Variation in the keratin refractive index estimated that values falling between 1.58 and 1.63 generated models that fall within the calculated CI (figure 6*a*, solid line). A melanin refractive index between 1.75 and 1.90 also improved the model fit (figure 6*b*, solid line). Combining both variations in the refractive index and the extinction coefficient further suggests that the changes in the refractive index are more relevant for obtaining a good model fit (table 3). Also, variation in hue values owing to changes in the angle of incident light remained fairly stable regardless of the changes in the melanin opacity, suggesting that the iridescent properties of the selected model are robust despite subtle variations in optical properties of the materials.

4. DISCUSSION

Male blue-black grassquit feather barbules present a single keratin layer over a layer comprising melanin granules. This simple arrangement is sufficient to produce iridescent coloration, as confirmed by thin-film optical modelling. Shifts in hue and shape of the reflected spectrum derived from changing angles of light incidence were well explained by the modelled differences in the optical path that light encounters at each angle. This result reinforces the conclusion that these barbules are photonic structures that interact with light as predicted by the thin-film models of refraction.

Thin-film optical modelling also revealed that light can only penetrate the melanin layer and interact with the keratin core when the melanin layer is sufficiently thin (fewer than two melanin granules, on average). Although this configuration can be found in some male grassquit feathers, most individuals have melanin layers of two to three granules, with little variation across average values. This suggests that plumage development in this species optimizes colour properties through the production and placement of sufficient granules to maximize absorbance, rarely generating more melanin granules than those strictly necessary for this colour production process. Therefore, the constructive interference of light in the single keratin layer, isolated from the core of the barbule by a sufficiently thick melanin layer, optimizes the reflection of short wavelengths (UV–blue) that produce the characteristic coloration of the nuptial plumage of male blue-black grassquits, without requiring any additional pigments or structures.

Several studies have described structures similar to those found in the blue-black grassquit, also by applying thin-film optical models. For instance, male
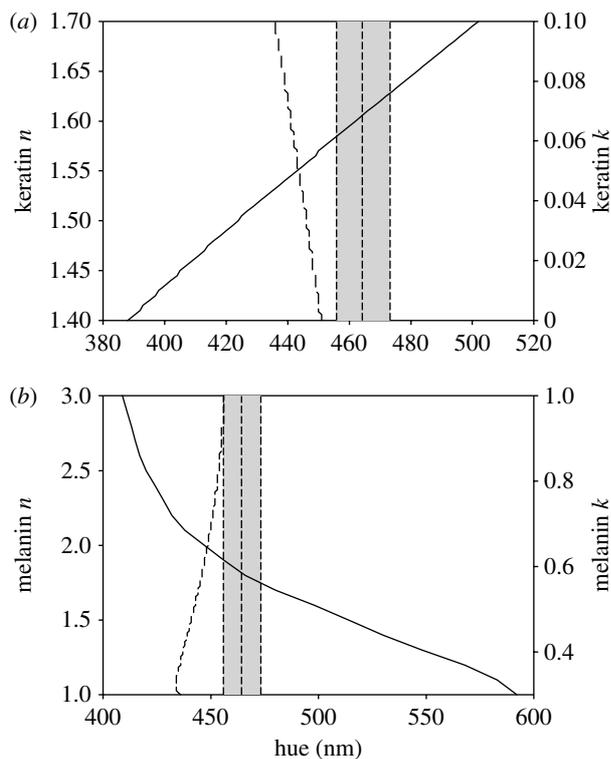
Figure 6. Predicted values of hue under normal incidence by thin-film optical models considering different values for the refractive index (n; solid lines) and the extinction coefficient (k; dashed lines) of (*a*) keratin and (*b*) melanin. Vertical dashed lines indicate the mean value of hue and its 95% CI (grey area), as estimated from the reflectance spectra obtained at normal incidence from feathers of male blue-black grassquits.

satin bowerbirds (Doucet *et al.* 2006), as well as some grackles and blackbirds (Shawkey *et al.* 2006), also produce iridescent colours with peak reflectance in short wavelengths owing to a keratin cortex over a single melanin layer. However, in other species such as the hadeda ibis (*Bostrychia hagedash*), the melanin platelets are hollow and could provide an extra inter-face between melanin and air, but the melanin was found to be highly opaque so that the resulting colour is produced by the keratin cortex alone (Brink & van der Berg 2004). The keratin layer in the barbules of this ibis is over four times thicker than that of male blue-black grassquits, resulting in a very different structural colour with up to four peaks in the avian visible spectra.

The role commonly attributed to melanin in the production of both iridescent and non-iridescent struc-tural colours is that of absorbing incoherently scattered light waves, therefore accentuating colour properties, especially saturation (Prum 2006; Shawkey & Hill 2006). The relationship found between the colour and melanin granule density in male satin bowerbirds (Doucet *et al.* 2006) is an example of this property in iridescent feathers. This is similar to the case of an amelanotic Steller's jay (*Cyanocitta stelleri*), which exhibits a non-iridescent blue colour. In this example, the absence of melanin in the quasi-ordered structure of feather barbs does not allow the absorbance of these incoherently scattered wavelengths, resulting in white-coloured feathers (Shawkey & Hill 2006).

The melanin layer is usually considered to have very little influence in coherent scattering and the resulting production of iridescent colours, absorbing most of the light that reaches it and therefore serving mostly to define the thickness of the keratin cortex (Brink & van der Berg 2004; Doucet *et al.* 2006). However, as shown for some cowbird species, if the melanin layer is sufficiently thin, light can interact with it and reach underlying layers (Shawkey *et al.* 2006). Similarly, in the blue-black grassquit, the melanin layer is relatively thin owing to the stacking of very few melanin granules. Indeed, variation in the number of melanin granules (i.e. layer thickness) found for males of this species may result in an altogether different organization of layers and interfaces interacting with light. Our data suggest that if the melanin layer is on average thinner than two melanin granules, light can reach the underlying melanin–keratin interface. The result is a change in the coherently reinforced wavelengths and, consequently, in the observed coloration. Thus, in accordance with the findings in species that display feathers with similar structures, the role of melanin in the nanostructural organization of blue-black grassquit feather barbs includes not only absorbance of incoherently reflected light, but also an active role in thin-film structural organization. The fact that the melanin substrate in iridescent feathers may absorb the most incident light does not mean that its relevance to colour production resides solely in this property. Its interface with the keratin cortex may also contribute to differential reinforcement of wavelengths when the melanin layer is sufficiently thin.

Our results also show that even considering the most adequate model selected by visual inspection, an improvement in model fit to empirical data can be achieved when optical properties of the materials are considered and changed. Ultimately, an ideal approach would be to objectively measure optical properties of keratin and melanin, using these values to generate predictive thin-film models. This also highlights the need for an objective methodology for comparing the predicted and empirically obtained colour spectra. The simple methodology applied in this study points to the potential traps of simply comparing colour curves visually. Also, we found that although peak reflectance changed, the overall distance between peak reflectance measured at both geometries (ΔHue) varied little with changes in opacity.

Altering the values of both materials' refractive index improved model fit by altering the optical path length ratio between the two layers (Kinoshita & Yoshioka 2005*b*). Thus, since melanin has a higher refractive index than keratin, it requires larger changes to achieve the necessary ratio to improve the model fit. Keratin is usually considered to have a refractive index of between 1.5 and 1.55, with Brink & van der Berg (2004) estimating values of 1.56–1.58 for the hadeda ibis. This renders our estimates even higher than most studies on insect cuticles and bird feathers. Melanin optical properties, on the other hand, have received considerably less attention, and little has changed since Land's (1972) suggestion of a refractive index of approximately 2.0. Brink & van der Berg (2004) tested

different values for the extinction coefficient in the hadeda ibis and suggested a minimal value of 0.6, in which the melanin layer width lies around 70 nm. We consider that taking a different value for the refractive index of melanin can be biologically more meaningful, since the optical properties available in the literature actually refer to eumelanin, but both eumelanin and phaeomelanin occur in all bird species studied to date (McGraw 2006b). Since phaeomelanin displays 10–30 per cent less absorbance in all wavelengths (Krishnaswamy & Baranoski 2004), a mixture of both would result in a change to the refractive index in the direction we have estimated, with little change to the extinction coefficient, for the difference in absorbance between the melanin types is somewhat consistent across wavelengths. Further studies should also consider that the differences in the amount of each type of melanin might even account for interspecific variation in estimated refractive indexes.

REFERENCES

Aguilar, T. M., Maia, R., Santos, E. S. A. & Macedo, R. H. 2008 Parasite levels in blue-black grassquits correlate with male displays but not female mate choice. *Behav. Ecol.* **19**, 292–301. (doi:10.1093/beheco/arm130)

Alonzo-Alvarez, C., Doutrelant, C. & Sorci, G. 2004 Ultraviolet reflectance affects male–male interactions in the blue tit (*Parus caeruleus ultramarinus*). *Behav. Ecol.* **15**, 805–809. (doi:10.1093/beheco/arh083)

Andersson, M. 1994 *Sexual selection*. Princeton, NJ: Princeton University Press.

Andersson, S. 1999 Morphology of UV reflectance in a whistling-thrush: implications for the study of color signaling in birds. *J. Avian Biol.* **30**, 193–204. (doi:10.2307/3677129)

Badyaev, A. V. & Hill, G. E. 2002 Paternal care as a conditional strategy: distinct reproductive tactics associated with elaboration of plumage ornamentation in the house finch. *Behav. Ecol.* **13**, 591–597. (doi:10.1093/beheco/13.5.591)

Bagnara, J. T., Fernandez, P. J. & Fuji, R. 2007 On the blue coloration of vertebrates. *Pigm. Cell Res.* **20**, 14–26. (doi:10.1111/j.1600-0749.2006.00360.x)

Banks, A. N. 2001 For your eyes only? The role of UV in mate choice. *Trends Ecol. Evol.* **16**, 473–474. (doi:10.1016/S0169-5347(01)02245-5)

Brink, D. J. & van der Berg, N. G. 2004 Structural colors from the feather of the bird *Bostrychia hagedash*. *J. Phys. D: Appl. Phys.* **37**, 813–818. (doi:10.1088/0022-3727/37/5/025)

Carvalho, C. B., Macedo, R. H. & Graves, J. 2006 Breeding strategies of a socially monogamous Neotropical passerine: extra-pair fertilizations, behavior and morphology. *Condor* **108**, 579–590. (doi:10.1650/0010-5422(2006)108[579:BSOASM]2.0.CO;2)

Costa, F. J. V. & Macedo, R. H. 2005 Coccidian oocyst parasitism in the blue-black grassquit: influence on secondary sex ornaments and body condition. *Anim. Behav.* **70**, 1401–1409. (doi:10.1016/j.anbehav.2005.03.024)

Cuthill, I. C. 2006 Color perception. In *Bird coloration* (eds G. E. Hill & K. J. McGraw). Mechanisms and measurements, vol. I, pp. 3–40. Cambridge, MA: Harvard University Press.

Cuthill, I. C., Partridge, J. C., Bennett, A. T. D., Church, S. C., Hart, N. S. & Hunt, S. 2000 Ultraviolet vision in birds. *Adv. Stud. Behav.* **29**, 159–214. (doi:10.1016/S0065-3454(08)60105-9)

Doucet, S. M. 2002 Structural plumage coloration, male body size, and condition in the blue-black grassquit. *Condor* **104**, 30–38. (doi:10.1650/0010-5422(2002)104[0030:SPCMBS]2.0.CO;2)

Doucet, S. M., Shawkey, M. D., Hill, G. E. & Montgomerie, R. 2006 Iridescent plumage in satin bowerbirds: structure, mechanisms and nanostructural predictors of individual variation in color. *J. Exp. Biol.* **209**, 380–390. (doi:10.1242/jeb.01988)

Eaton, M. D. & Lanyon, S. M. 2003 The ubiquity of avian ultraviolet plumage reflectance. *Proc. R. Soc. B* **270**, 1721–1726. (doi:10.1098/rspb.2003.2431)

Figuerola, J., Munoz, E., Gutierrez, R. & Ferrer, D. 1999 Blood parasites, leucocytes and plumage brightness in the cirl bunting, *Emberiza cirlus. Funct. Ecol.* **13**, 594–601. (doi:10.1046/j.1365-2435.1999.00354.x)

Greenwalt, C. H., Brandt, W. & Friel, D. D. 1960 Iridescent colors of hummingbird feathers. *J. Opt. Soc. Am.* **50**, 1005–1013. (doi:10.1364/JOSA.50.001005)

Håstad, O. & Ödeen, A. 2008 Different ranking of avian colors predicted by modeling of retinal function in humans and birds. *Am. Nat.* **171**, 831–838. (doi:10.1086/587529)

Haussmann, F., Arnold, K. E., Marshall, N. J. & Owens, I. P. F. 2003 Ultraviolet signals in bird are special. *Proc. R. Soc. B* **270**, 61–67. (doi:10.1098/rspb.2002.2200)

Jellison Jr, G. E. 1993 Data analysis for spectroscopic ellipsometry. *Thin Solid Films* **234**, 416–422. (doi:10.1016/0040-6090(93)90298-4)

Kinoshita, S. & Yoshioka, S. 2005a Fundamental optical processes underlying the structural colors. In *Structural colors in biological systems: principles and applications* (eds S. Kinoshita & S. Yoshioka), pp. 3–26. Osaka, Japan: Osaka University Press.

Kinoshita, S. & Yoshioka, S. 2005b Structural colors in nature: a role of regularity and irregularity in the structure. *ChemPhysChem* **6**, 1443–1459. (doi:10.1002/cphc.200500007)

Kinoshita, S., Yoshioka, S. & Miyazaki, J. 2008 Physics of structural colors. *Rep. Prog. Phys.* **71**, 076401(1-30). (doi:10.1088/0034-4885/71/7/076401)

Krishnaswamy, A. & Baranoski, G. V. G. 2004 A biophysically-based spectral model of light interaction with human skin. *Comp. Graph. Forum* **23**, 331–340. (doi:10.1111/j.1467-8659.2004.00764.x)

Land, M. F. 1972 The physics and biology of animal reflectors. *Prog. Biophys. Mol. Biol.* **24**, 77–106. (doi:10.1016/0079-6107(72)90004-1)

McGraw, K. J. 2006a Mechanics of carotenoid-based coloration. In *Bird coloration* (eds G. E. Hill & K. J. McGraw). Mechanisms and measurements, vol. I, pp. 177–242. Cambridge, MA: Harvard University Press.

McGraw, K. J. 2006*b* Mechanics of melanin-based coloration. In *Bird coloration* (eds G. E. Hill & K. J. McGraw). Mechanisms and measurements, vol. I, pp. 243–294. Cambridge, MA: Harvard University Press.

McGraw, K. J. 2006*c* Mechanics of uncommon colors: pterins, porphyrins and psittacofulvins. In *Bird coloration* (eds G. E. Hill & K. J. McGraw). Mechanisms and measurements, vol. I, pp. 354–398. Cambridge, MA: Harvard University Press.

Osorio, D. & Ham, A. D. 2002 Spectral reflectance and directional properties of structural coloration in bird plumage. *J. Exp. Biol.* **205**, 2017–2027.

Prum, R. O. 2006 Anatomy, physics, and evolution of avian structural colors. In *Bird coloration* (eds G. E. Hill & K. J. McGraw). Mechanisms and measurements, vol. I, pp. 295–355. Cambridge, MA: Harvard University Press.

Prum, R. O. & Torres, R. H. 2003 A Fourier tool for the analysis of coherent light scattering by bio-optical nanostructures. *Integr. Comp. Biol.* **43**, 591–602. (doi:10.1093/icb/43.4.591)

Prum, R. O., Torres, R., Williamson, S. & Dyck, J. 1998 Constructive inference of light by blue feather barbs. *Nature* **396**, 28–29. (doi:10.1038/23838)

Rasband, W. S. 1997–2007 IMAGE J. Bethesda, MD: US National Institutes of Health. See http://rsb.info.nih.gov/ij/.

R Development Core Team 2007 *R: a language for data analysis and graphics.* Vienna, Austria: R Foundation for Statistical Computing. See http://cran.r-project.org/.

Searcy, W. & Nowiki, S. 2005 *The evolution of animal communication.* Princeton, NJ: Princeton University Press.

Shawkey, M. D. & Hill, G. E. 2006 Significance of a basal melanin layer to production of non-iridescent structural plumage color: evidence from an amelanotic Steller's jay (*Cyanocitta stelleri*). *J. Exp. Biol.* **209**, 1245–1250. (doi:10.1242/jeb.02115)

Shawkey, M. D., Hauber, M. E., Estep, L. K. & Hill, G. E. 2006 Evolutionary transitions and structural mechanisms of avian plumage coloration in grackles and allies (Icteridae). *J. R. Soc. Interface* **3**, 777–783. (doi:10.1098/rsif.2006.0131)

Shawkey, M. D., Saranathan, V., Palsdottir, H., Crum, J., Ellisman, M. H., Auer, M. & Prum, R. O. In press. Electron tomography, 3D Fourier analysis and color prediction of a 3D amorphous bio-photonic nanostructure. *J. R. Soc. Interface.*

Srinivasarao, M. 1999 Nano-optics in the biological world: beetles, butterflies, birds and moths. *Chem. Rev.* **99**, 1935–1961. (doi:10.1021/cr970080y)

Webber, T. 1985 Songs, displays and other behavior at a courtship gathering of blue-black grassquit. *Condor* **87**, 543–546. (doi:10.2307/1367957)

Yin, H., Shi, L., Li, Y., Quin, Y., Dong, B., Meyer, S., Liu, X., Zhao, L. & Zi, J. 2006 Iridescence in the neck feathers of domestic pigeons. *Phys. Rev. E* **72**, 051916(1-6). (doi:10.1103/PhysRevE.74.051916)

Yoshioka, S., Nakamura, E. & Konoshita, S. 2007 Origin of two-color iridescence in rock dove's feather. *J. Phys. Soc. Jpn* **76**, 013801(1-4). (doi:10.1143/JPSJ.76.013801)

Yoshioka, S., Nakano, T., Nozue, Y. & Kinoshita, S. 2008 Coloration using higher order optical interference in the wing pattern of the Madagascan sunset moth. *J. R. Soc. Interface* **5**, 457–464. (doi:10.1098/rsif.2007.1268)

Zi, J., Yu, X., Li, Y., Hu, X., Xu, C., Wang, X., Liu, X. & Fu, R. 2003 Coloration strategies in peacock feathers. *Proc. Natl Acad. Sci. USA* **100**, 12 576–12 578. (doi:10.1073/pnas.2133313100)